IAES International Journal of Robotics and Automation (IJRA)
Vol. 15, No. 4, December 2026, pp. 810~819
ISSN: 2722-2586, DOI: 10.11591/ijra.v15i4.pp810-819

Cost-effective four-axis CNC router with real-time monitoring

Eman Ebrahim, Ibrahim Al Souleiman
Swiss International University (SIU), Zurich, Switzerland

Article Info

Article history:

Received Jul 15, 2026
Revised Sep 3, 2026
Accepted Nov 10, 2026

Keywords:

CNC router
Four-axis machining
Kinematics
Robotics and automation
Structural analysis

ABSTRACT

This study presents the design, fabrication, and validation of a low-cost four-axis computer numerical control (CNC) router for educational laboratories, maker spaces, and light prototyping. The machine combines X, Y, and Z linear motion with a rotary A-axis, NEMA 23 stepper drives, TB6600 drivers, an ESP32 controller running FluidNC, an 800 W spindle, safety sensors, and a browser-based 3D visualization interface. The platform is framed as an automation and robotics system with a four-axis kinematic model, actuator-load equations, a control architecture, a reproducible measurement protocol, and a traceable structural-analysis discussion. The prototype achieved a linear positioning tolerance of ±0.05 mm and rotary positioning tolerance of ±0.5°, produced printed circuit board (PCB) isolation features down to 0.3 mm trace width and 0.2 mm spacing, and completed continuous four-hour operation without step loss or communication failure. The four-axis configuration expanded machining flexibility by enabling wrap-around machining of cylindrical workpieces. Because the original experimental record did not retain replicate-level measurements or complete finite element analysis (FEA) solver inputs, the manuscript explicitly distinguishes verified reported results from parameters requiring re-measurement. This limitation is used to define a transparent validation protocol rather than introduce fabricated statistics.

This is an open access article under the CC BY-SA license.

Corresponding Author:

Eman Ebrahim
Swiss International University (SIU)
Switzerland, Zurich
Email: dr.n.eman@swiss.edu.eu

1. INTRODUCTION

Computer numerical control (CNC) machines are cyber-physical manufacturing systems in which mechanical motion, embedded control, sensing, and software are coordinated to execute tool trajectories. This integration places CNC platforms directly within robotics and automation because the machine converts digital task descriptions into coordinated multi-axis motion while monitoring safety and process state [1], [2]. Recent work has emphasized open-architecture controllers, machine-tool accuracy modeling, multisensory error assessment, and digitalized monitoring as routes toward more accessible and intelligent manufacturing systems [3]–[7]. Open architectures are particularly attractive for education and prototyping. STEP-NC-based control, low-cost embedded controllers, and modular motion-control architectures demonstrate that the CAD/CAM/controller chain can be implemented with accessible computing hardware while retaining a clear automation structure [1], [8]. At the same time, accuracy remains governed by geometric errors, assembly deviations, thermal effects, dynamic loading, and the interaction between mechanical and control subsystems [3]–[6], [9]. Real-time monitoring is another important direction. Multisensory error analysis, energy-based operation monitoring, and digital-twin research show how machine state can be connected to higher-level software for diagnosis, visualization, and future predictive functions [2], [10]–[14]. However, a browser visualization that only mirrors current machine coordinates should not be described as a full digital twin.

Digital-twin implementations require defined relationships between the physical asset, digital model, data, and services; predictive or bidirectional functions are typically additional levels of maturity [11]–[14]. Therefore, this work uses the term "3D Visualization System" for the implemented interface. Despite these advances, a practical gap remains between expensive commercial four-axis systems and educational or maker environments where budget, maintainability, and transparency of the control stack are critical. The contribution is the integration of a low-cost four-axis mechatronic mechanism, embedded motion control, safety sensing, and real-time visualization into one automation platform. The rotary attachment extends machining to cylindrical workpieces, while the ESP32/FluidNC architecture is accessible for experimentation with motion control, communication, sensing, and future intelligent functions. Accordingly, the scientific question is whether a low-cost four-axis CNC platform can provide a quantitatively defined and practically useful combination of kinematic flexibility, positioning accuracy, structural adequacy, and real-time monitoring for educational and maker-oriented automation. The available prototype evidence reports ±0.05 mm linear and ±0.5° rotary positioning tolerances while completing representative printed circuit board (PCB), wood, and cylindrical machining tasks. The evidence consists of calibration tests, machining demonstrations, emergency-stop testing, continuous-operation tests, and SolidWorks structural simulations. The broader significance is a transparent automation platform that can support control engineering, sensor integration, and future predictive maintenance research without requiring a commercial industrial controller.

2. THE PROPOSED METHOD/ALGORITHM/PROCEDURE

2.1. System concept and kinematic representation

The proposed machine is modeled as a Cartesian three-axis stage augmented by a rotary A-axis, as in Figure 1. The generalized coordinate vector is $q = [x, y, z, \theta_A]^T$. The linear axes determine tool translation and the A-axis rotates a cylindrical workpiece. This representation makes the platform directly interpretable as a four-degree-of-freedom automated manipulator for machining.

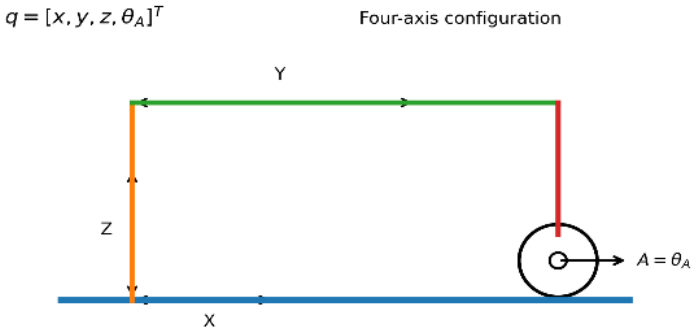

Figure 1. Kinematic representation of the four-axis CNC platform used for the revised robotics-oriented analysis

For a rotary axis defined about the machine Y-axis, the homogeneous transformation is:

$$T(q) = Trans(x, y, z) \cdot Rot_Y(\theta A)$$

For the Cartesian arrangement, inverse position mapping is direct for the translational coordinates,

$$x = x_d, y = y_d, z = z_d$$

while the required rotary command is

$$\theta_A = \theta_d$$

Step conversion is:

$$N_x = \frac{x \cdot S_x}{L_x}, \quad N_y = \frac{y \cdot S_y}{L_y}, \quad N_z = \frac{z \cdot S_z}{L_z}, \quad N_A = \frac{\theta_A \cdot (N_\mu \cdot 200)}{360}$$

where L is lead per revolution, S is the microstep setting, Nμ is the microstepping multiplier, and 200 is the number of full steps per revolution for 1.8° NEMA 23 motors. This links the physical transmission directly to FluidNC steps-per-mm and rotary-axis calibration.

2.2. Actuator and dynamic-load model

The mechanical sizing was interpreted using a quasi-static and acceleration-aware actuator model. For a linear axis, the motor torque requirement can be written as:

$$T_{req} = \frac{F_a \cdot L}{2\pi\eta} + J_{eq} \cdot \alpha + T_f$$

where F_a is axis force, L is screw lead, η is transmission efficiency, J_{eq} is reflected rotational inertia, α is angular acceleration, and T_f represents friction and parasitic torque. The available motor torque must exceed T_{req} with a suitable design margin. Cutting force should include cutting, friction, gravity for the Z-axis, and acceleration loads [3], [9]. The original manuscript reported 3.0 N·m holding torque for the NEMA 23 motors and an 800 W spindle. Because cutting-force measurements were not retained, this revision does not assign an unsupported numerical cutting force.

2.3. Automated control and monitoring procedure

The proposed procedure follows an information loop: CAD/CAM defines the task, the web application processes or forwards the motion program, FluidNC executes coordinated motion on the ESP32, the drivers energize the four stepper axes, and limit/probe/emergency inputs provide safety-state information. Position and machine state are returned to the visualization layer. This procedure is visualized in Figure 2. The operational workflow is summarized in Figure 3. Separation of deterministic motion control from higher-level visualization reduces the risk that browser-level tasks interrupt time-sensitive step generation.

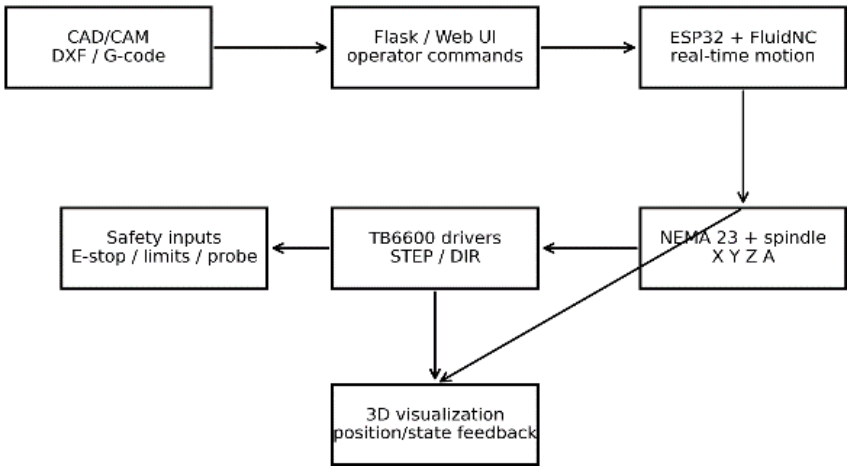

Figure 2. Integrated mechanical, control, sensing, and monitoring architecture of the proposed automation platform

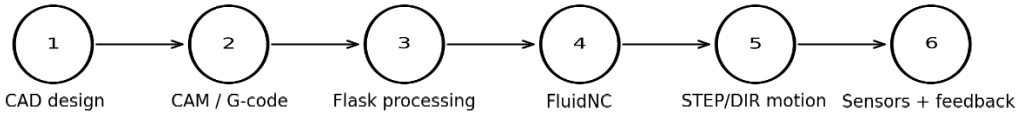

Figure 3. Automated workflow from CAD/CAM input to four-axis motion and sensor-state feedback

3. METHOD

3.1. Mechanical design and system specifications

The mechanical design used aluminum extrusion profiles, guide rails and bearing blocks, lead-screw transmission, a moving gantry, an MDF work surface, a spindle holder, and a rotary A-axis. Figure 4 shows

the complete CAD assembly. Component descriptions are condensed into Table 1 to avoid repeating textbook functions.

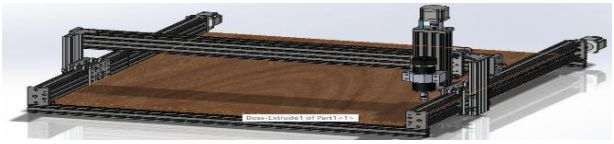

Figure 4. Complete CAD assembly of the four-axis CNC router used as the basis of the prototype

Table 1. Component descriptions

Parameter	Specification
Machine type	Four-axis CNC router
Axes	X, Y, Z linear + A rotary
Frame	Aluminum extrusion profiles
Transmission	Lead screws
Linear guidance	Guide rails and bearing blocks
Actuators	NEMA 23, 1.8°, 3.0 N·m holding torque
Drivers	TB6600, up to 4 A class
Controller	ESP32-DevKitC + FluidNC
Spindle	800 W DC air-cooled
Power	24 V / 20 A motion supply; separate spindle supply
Design software	SolidWorks
CAM/control	FlatCAM, FluidNC, Python/Flask, browser UI
Applications	PCB isolation, engraving, drilling, light profiling, rotary machining

3.2. Structural analysis and FEA methodology

SolidWorks simulation static studies were used in the original design to screen stress concentrations, displacement, and factor of safety. Figures 5 to 7 reproduce the available solver outputs. The reported minimum factor of safety was 1.50, while localized von Mises stress was reported in the range 115.4 to 185.7 MPa.

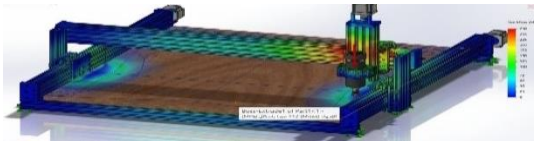

Figure 5. Available von Mises stress result for the complete machine assembly

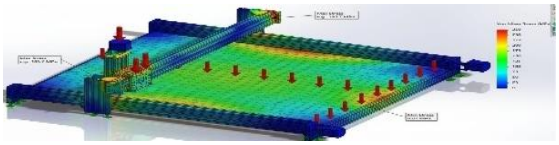

Figure 6. Available stress result showing load distribution over the worktable and gantry

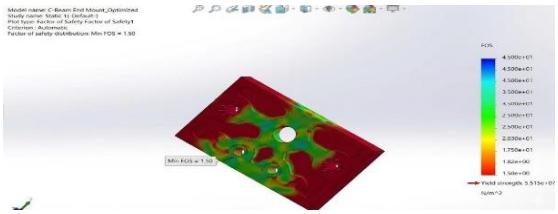

Figure 7. Available factor-of-safety result for the C-beam end mount; reported minimum FOS = 1.50

A major reproducibility issue identified during revision is that the original manuscript retained contour plots but not the solver report containing boundary conditions, element type, mesh statistics, exact applied cutting forces, and material cards. These values cannot be reconstructed reliably from a contour image. Table 2 therefore separates traceable information from missing inputs; the revision intentionally does not invent numerical forces or mesh settings.

Table 2. Traceable information from missing inputs

FEA item	Traceable from original record	Required for reproducible rerun
Software	SolidWorks Simulation	Version and study type
Analysis	Static structural screening	Load-case definition
Boundary conditions	Supports visible in model images	Exact fixed/fixture faces and constraints
Applied load	Cutting/distributed loading shown qualitatively	Force magnitude and direction in N for each load case
Material	Aluminum structural members reported	Exact alloy/temper and material-card properties
Mesh	Not retained in manuscript	Element type, global size, local refinement, convergence criterion
Outputs	115.4–185.7 MPa stress; minimum FOS 1.50	Recomputed stress, displacement, and FOS after rerun

For final publication, the original SolidWorks study report should be attached or the finite element analysis (FEA) should be rerun with the as-built CAD model. The rerun should record alloy and Young's modulus, Poisson's ratio and yield strength; fixed faces; cutting-force components in N; mesh type and size; and mesh-convergence results.

3.3. Electronics, isolation, and safety

The ESP32 generates STEP/DIR commands for four TB6600 drivers, controls spindle speed through PWM, and reads limit, probe, and emergency-stop states. A custom KiCad PCB was used as the interface layer. The original design included optocouplers and buffer circuitry; this isolation approach is retained as a key safety and signal-integrity feature.

Because the original manuscript did not include the final FluidNC YAML or a pinout table, exact GPIO-to-driver mapping cannot be stated without risk of recording an incorrect as-built configuration. The final reproducibility package should include the actual configuration file and the following traceability matrix.

The machine is intended for supervised educational use. Emergency-stop function, axis limits, spindle guarding, cable management, and low-energy training cuts should be verified before student operation. The physical emergency-stop path should remain independent of the browser interface. The signal groups, their functions, and the corresponding sources for verification are summarized in Table 3.

Table 3. Signal group functions and sources of verification

Signal group	Function	Source to verify before submission
X STEP/DIR	X-axis motion	As-built FluidNC YAML
Y STEP/DIR	Y-axis motion	As-built FluidNC YAML
Z STEP/DIR	Z-axis motion	As-built FluidNC YAML
A STEP/DIR	Rotary-axis motion	As-built FluidNC YAML
PWM	Spindle speed command	As-built FluidNC YAML
Limits	Homing/overtravel protection	As-built FluidNC YAML
Probe	Z-zero detection	As-built wiring + YAML
E-stop	Emergency stop / power inhibit	As-built wiring diagram

3.4. Software configuration and monitoring

FluidNC was selected because it is designed for ESP32-based CNC control and supports machine definitions through a configuration file. The control stack comprises the ESP32/FluidNC motion layer, Python/Flask middleware, and browser-based visualization. The original implementation used an approximately 80 ms polling interval. The browser interface is called a 3D visualization system rather than a digital twin because the implemented function is descriptive visualization rather than a validated bidirectional predictive model [11]–[14]. The architecture is suitable for later expansion toward Internet of Things (IoT) monitoring, sensor fusion, predictive maintenance, and closed-loop control [2], [10], [15]–[19].

3.5. Experimental protocol and measurement validation

The original accuracy claim was obtained by commanding a 100 mm move on each linear axis and comparing commanded and actual displacement using a digital caliper; the A-axis was commanded through 360° and checked for angular displacement. The original record did not retain the caliper model/resolution, ambient temperature, humidity, number of replicate trials, individual readings, or uncertainty budget. Therefore, ±0.05 mm and ±0.5° are retained as reported prototype tolerances, not newly calculated statistical estimates. Table 4 summarizes the measurements and proposed repeatability protocol.

Table 4. Reported measurement results and recommended repeatability protocol

Validation item	Original reported result	Required repeatability protocol
Linear travel	100 mm command; ±0.05 mm reported tolerance	≥10 repetitions/axis at 25, 50, 75 and 100 mm; record each reading
Rotary travel	360° command; ±0.5° reported tolerance	≥10 repetitions at 90°, 180°, 270° and 360°
Instrument	Digital caliper reported	Record make/model and resolution; use calibrated angular reference
Environment	Not recorded	Record temperature, humidity and machine warm-up time
Statistics	Raw replicates unavailable	Report mean error, SD, maximum absolute error and 95% CI
Acceptance	±0.05 mm linear; ±0.5° rotary	Compare each axis and direction against predefined tolerance

For commanded distance d_i and measured distance m_i, signed error is $e_i = m_i - d_i$. The mean error, sample standard deviation and approximate 95% confidence interval are:

$$\bar{e} = \frac{1}{n}\sum e_i\,; \quad s = \sqrt{\frac{\sum(e_i - \bar{e})^2}{n-1}}; \quad CI_{95} \approx \bar{e} \pm t_{0.975,n-1} \cdot \frac{s}{\sqrt{n}}$$

3.6. Cost and benchmark framework

The cost-effectiveness claim is evaluated as a system-level proposition. Table 5 provides an indicative prototype allocation to show where cost is concentrated. These values are engineering estimates for benchmarking only, not audited purchase records; the final submission should replace them with actual invoices or a build log.

The benchmark is not only purchasing price but also control transparency, maintainability, and educational value. Commercial four-axis systems generally integrate industrial motion controllers, enclosed mechanics, higher-duty spindles, and calibrated metrology, so direct price equivalence would be misleading. The contribution is the combination of low-cost open architecture, a fourth axis, and real-time visualization in a platform whose internal control chain can be inspected and modified.

Table 5. Indicative prototype allocation

Subsystem	Indicative USD	Share
Frame, extrusion, rails and bearings	180	24%
Lead screws and couplings	90	12%
NEMA 23 motors and TB6600 drivers	140	19%
800 W spindle and power hardware	120	16%
ESP32, PCB, isolation and wiring	70	9%
A-axis, safety and sensors	90	12%
Fasteners, cable management and misc.	60	8%
Illustrative prototype total	750	100%

4. RESULTS AND DISCUSSION

4.1. Positioning performance

The available prototype results indicate ±0.05 mm linear positioning tolerance over the tested range and ±0.5° rotary positioning tolerance after calibration. These values should be interpreted as positioning tolerance under the reported test condition, not as certified volumetric accuracy or repeatability. Modern machine-tool literature shows that geometric, assembly, thermal, and load-dependent errors can influence accuracy [3]–[7], [9], [20].

Figure 8 shows the prototype during operation. The practical value of the fourth axis is demonstrated by wrap-around machining of cylindrical workpieces, reducing repeated re-fixturing and expanding reachable geometry compared with a three-axis setup. Table 6 summarizes the prototype's reported performance and operational test results.

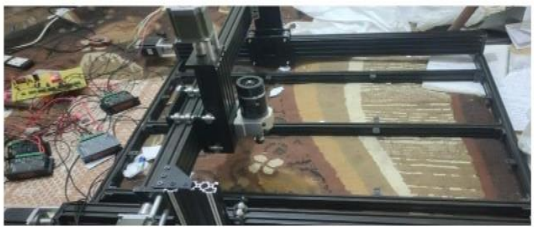

Figure 8. Prototype CNC router during machining and monitoring tests

Table 6. Summary of prototype performance and operational test results

Metric	Reported value	Interpretation
Linear positioning tolerance	±0.05 mm	Prototype calibration result; replicate-level SD unavailable
Rotary positioning tolerance	±0.5°	Prototype A-axis calibration result; replicate-level SD unavailable
PCB feature	0.3 mm trace width; 0.2 mm spacing	Demonstrated isolation-milling capability
Maximum configured feed rate	1000 mm/min	Used in emergency-stop test
Emergency stop	<1 mm reported stop distance	Feed-hold response under stated configuration
Continuous operation	4 h	No reported step loss, overheating or communication failure

4.2. Machining flexibility and automation significance

The four-axis configuration improves flexibility because the rotary workpiece axis changes the machining setup from repeated indexed fixtures toward continuous or indexed cylindrical toolpaths. From a robotics perspective, the additional degree of freedom changes the configuration space and allows a larger class of task trajectories without changing the physical fixture. The platform therefore serves as a small-scale manufacturing robot with deterministic trajectory execution.

The automation value also arises from separation of layers. FluidNC handles time-sensitive motion, Flask handles supervisory communication, and the browser provides human-readable state information. This layered approach is consistent with open-architecture CNC research and creates a pathway to sensor fusion and intelligent diagnosis [1], [2], [8], [10].

4.3. Monitoring, safety, and terminology

The original interface provided real-time 3D visualization of machine state. The available evidence supports descriptive visualization, not a complete digital twin. Recent digital-twin studies emphasize physical-to-digital relationships, model fidelity, and service-level functions such as diagnosis, prediction, or virtual commissioning [11]–[14], [21]. Renaming the implemented feature to “3D Visualization System” improves technical accuracy while preserving real-time operator awareness.

The monitoring layer also has a safety role: the operator can observe commanded and reported position, while hardwired limit and emergency-stop functions provide independent protection. The browser interface must never be treated as the primary safety mechanism, especially in educational laboratories.

4.4. Comparison with related research

Compared with open-architecture CNC controllers, the present platform emphasizes low-cost four-axis mechanical integration plus supervisory visualization [1], [8]. Compared with high-precision CNC metrology studies, its ±0.05 mm result is modest and should not be interpreted as an industrial accuracy class [3]–[7], [20]. Compared with intelligent monitoring and digital-twin studies, the present system is at an earlier descriptive level but provides a physically accessible platform on which energy, vibration, temperature, current, or tool-wear sensors can be added [10]–[19], [21]–[23].

The novelty is not a new motion-control algorithm. It is the integrated low-cost automation architecture that combines a four-axis mechanism, embedded control, safety sensing, and real-time visualization with an explicit robotics-oriented kinematic and load model. The platform is consequently valuable as an open experimental system for education, rapid prototyping, and future intelligent manufacturing research.

4.5. Limitations and reproducibility

Three limitations constrain the strength of the evidence. First, the prototype was evaluated in a limited set of materials and machining conditions; large-scale industrial validation was not performed. Second, replicate-level metrology data were not preserved, preventing a defensible calculation of standard

deviation, confidence intervals, and statistical repeatability. Third, the archived FEA plots do not contain the complete solver input set, and the exact FluidNC GPIO mapping and YAML parameters were not retained. These limitations are explicitly disclosed because adding invented numerical values would weaken scientific validity.

The next validation campaign should log raw measurements, instrument specifications, ambient conditions, cutting-force data, spindle speed, feed rate, material, tool geometry, and complete FluidNC configuration. CAD, KiCad, and software files should be released in a public repository where permitted to support independent replication.

4.6. Cost-effectiveness and broader impact

The low-cost architecture exposes the full automation stack to students and makers: mechanical transmission, kinematics, embedded control, signal isolation, sensor inputs, communication, visualization, and CAM. This supports laboratory exercises in robotics, control engineering, mechatronics, sensor technologies, and manufacturing systems. The platform can also be extended toward IoT monitoring and predictive maintenance, where recent work has shown the value of multisensor data and machine learning for tool and machine condition assessment [10], [15]–[19], [22], [23].

4.7. Future research direction

Future work should validate the machine across aluminum, polymers, wood, composites, and additional tool geometries using repeated measurements and controlled cutting forces. Closed-loop stepper or servo drives with encoders should be added to detect and correct step loss. Vibration, spindle current, temperature, acoustic emission, and tool-wear sensors should be integrated for predictive maintenance and adaptive feed control [15]–[19], [22], [23]. Finally, the 3D visualization system can evolve into a standards-aware digital twin with bidirectional data, physics-based or data-driven models, and predictive functions [11]–[14], [21], [24], [25]. Classroom and maker-space trials should quantify usability, learning outcomes, safety compliance, and maintenance burden.

5. CONCLUSION

This revised study reframed a low-cost four-axis CNC router as an integrated robotics and automation platform rather than a component-level construction report. The system combined X–Y–Z translation and A-axis rotation with NEMA 23 stepper actuators, TB6600 drivers, an ESP32/FluidNC controller, safety sensing, and a browser-based 3D visualization layer. The available prototype evidence reported ±0.05 mm linear positioning tolerance, ±0.5° rotary positioning tolerance, PCB isolation capability down to 0.3 mm trace width with 0.2 mm spacing, less than 1 mm reported emergency-stop distance at the tested feed condition, and stable four-hour operation. The kinematic and actuator-load models clarify the relationship between commanded motion, transmission parameters, and mechanical loading, while the revised FEA discussion explicitly separates traceable results from missing solver inputs. The main scientific advance is an accessible, modular automation architecture that exposes the interaction of mechanical design, motion control, sensing, communication, and visualization in one four-axis manufacturing platform. Its broader value is in control-engineering education, sensor integration, rapid manufacturing prototyping, and future intelligent-machine research. The principal limitations are prototype-scale validation, missing replicate-level raw metrology data, incomplete archived FEA inputs, and the absence of industrial closed-loop control. Future work will address these limitations through statistically designed repeated measurements, verified FEA reruns, open release of CAD/KiCad/software artifacts, IoT-enabled sensing, predictive maintenance, adaptive control, and classroom/maker-space validation.

FUNDING INFORMATION

Authors state no funding involved.

AUTHOR CONTRIBUTIONS STATEMENT

This journal uses the Contributor Roles Taxonomy (CRediT) to recognize individual author contributions, reduce authorship disputes, and facilitate collaboration.

Name of Author	C	M	So	Va	Fo	I	R	D	O	E	Vi	Su	P	Fu
Eman Ebrahim	✓	✓	✓	✓	✓	✓		✓	✓	✓			✓	
Ibrahim Al Souleiman		✓				✓		✓	✓	✓	✓	✓		

C : **C**onceptualization	I : **I**nvestigation	Vi : **Vi**sualization
M : **M**ethodology	R : **R**esources	Su : **Su**pervision
So : **So**ftware	D : **D**ata Curation	P : **P**roject administration
Va : **Va**lidation	O : Writing - **O**riginal Draft	Fu : **Fu**nding acquisition
Fo : **Fo**rmal analysis	E : Writing - Review & **E**diting	

CONFLICT OF INTEREST STATEMENT

Authors state no conflict of interest.

REFERENCES

[1] M. Dharmawardhana, A. Ratnaweera, and G. Oancea, "Step-nc compliant intelligent cnc milling machine with an open architecture controller," *Applied Sciences (Switzerland)*, vol. 11, no. 13, p. 6223, 2021, doi: 10.3390/app11136223.

[2] X. Li, Y. Deng, and X. Li, "Application of multisensor information fusion technology in the measurement of dynamic machining errors of computer numerical control (CNC) machine tools," *Journal of Sensors*, vol. 2021, p. 6918496, 2021, doi: 10.1155/2021/6918496.

[3] Z. Wang and H. Yuan, "Enhancing machining accuracy reliability of multi-axis cnc machine tools using an advanced importance sampling method," *Eksploatacja i Niezawodnosc*, vol. 23, no. 3, pp. 559–568, 2021, doi: 10.17531/EIN.2021.3.17.

[4] P. L. Liu, Z. C. Du, H. M. Li, M. Deng, X. B. Feng, and J. G. Yang, "Thermal error modeling based on BiLSTM deep learning for CNC machine tool," *Advances in Manufacturing*, vol. 9, no. 2, pp. 235–249, 2021, doi: 10.1007/s40436-020-00342-x.

[5] Y. Hu, J. Zhu, and M. Chen, "State-of-the-art of on-machine measurement technology for NC machining accuracy," *Machine Tool \& Hydraulics*, vol. 49, no. 16, pp. 168–173, 2021, doi: 10.3969/j.issn.1001-3881.2021.16.035.

[6] S. Guo, J. Yang, G. Qiao, and X. Mei, "Assembly deviation modelling to predict and trace the geometric accuracy of the precision motion system of a CNC machine tool," *Mechanism and Machine Theory*, vol. 169, p. 104687, 2022, doi: 10.1016/j.mechmachtheory.2021.104687.

[7] J. Švéda, Š. Chládek, T. Hornych, T. Kozlok, and J. Smolík, "Increasing machining accuracy based on CNC machine tool correction data by using ad hoc modification," *Machines*, vol. 10, no. 5, p. 288, 2022, doi: 10.3390/machines10050288.

[8] V. Selvaraj, Z. Xu, and S. Min, "Intelligent operation monitoring of an ultra-precision CNC machine tool using energy data," *International Journal of Precision Engineering and Manufacturing - Green Technology*, vol. 10, no. 1, pp. 59–69, 2023, doi: 10.1007/s40684-022-00449-5.

[9] H. Huang, J.-R. Li, and D.-L. Li, "Design of virtual and real interactive monitoring system for CNC machine tools based on digital twins," *Journal of Lanzhou University of Technology*, vol. 49, no. 1, pp. 36–43, 2023.

[10] Z. Feng, X. Min, W. Jiang, F. Song, and X. Li, "Study on thermal error modeling for CNC machine tools based on the improved radial basis function neural network," *Applied Sciences (Switzerland)*, vol. 13, no. 9, p. 5299, 2023, doi: 10.3390/app13095299.

[11] Y. Gao, X. Xia, and Y. Guo, "A modeling method for thermal error prediction of CNC machine equipment based on sparrow search algorithm and long short-term memory neural network," *Sensors*, vol. 23, no. 7, p. 3600, Mar. 2023, doi: 10.3390/s23073600.

[12] J. Peng, M. Yin, L. Cao, L. F. Xie, X. J. Wang, and G. F. Yin, "Study on the thermally induced spindle angular errors of a five-axis CNC machine tool," *Advances in Manufacturing*, vol. 11, no. 1, pp. 75–92, 2023, doi: 10.1007/s40436-022-00409-x.

[13] Y. Li, Y. Zhang, and N. An, "Accuracy reliability analysis of CNC machine tools considering manufacturing errors degrees," *Proceedings of the Institution of Mechanical Engineers, Part O: Journal of Risk and Reliability*, vol. 238, no. 3, pp. 643–653, 2024, doi: 10.1177/1748006X231153704.

[14] F. Gougam, A. Afia, M. A. Aitchikh, W. Touzout, C. Rahmoune, and D. Benazzouz, "Computer numerical control machine tool wear monitoring through a data-driven approach," *Advances in Mechanical Engineering*, vol. 16, no. 2, 2024, doi: 10.1177/16878132241229314.

[15] C. Dong and J. Zhao, "An augmented autoencoder with multi-head attention for tool wear prediction in smart manufacturing," *IEEE Access*, vol. 12, pp. 79128–79137, 2024, doi: 10.1109/ACCESS.2024.3406568.

[16] X. Wang, D. Zhang, and Z. Zhang, "A review of dynamics design methods for high-speed and high-precision CNC machine tool feed systems." 2023. [Online]. Available: http://arxiv.org/abs/2307.03440

[17] J. E. Correa, N. Toombs, and P. M. Ferreira, "A modular-architecture controller for CNC systems based on open-source electronics," *Journal of Manufacturing Systems*, vol. 44, no. 3, pp. 317–323, 2017, doi: 10.1016/j.jmsy.2017.04.013.

[18] G. Sa *et al.*, "A digital twin synchronous evolution method of CNC machine tools associated with dynamic and static errors," *International Journal of Advanced Manufacturing Technology*, vol. 134, no. 5–6, pp. 2753–2763, 2024, doi: 10.1007/s00170-024-14244-w.

[19] K. Li, Z. Li, X. Jia, L. Liu, and M. Chen, "A domain adversarial graph convolutional network for intelligent monitoring of tool wear in machine tools," *Computers and Industrial Engineering*, vol. 187, p. 109795, 2024, doi: 10.1016/j.cie.2023.109795.

[20] Y. Pan, L. Hao, J. He, K. Ding, Q. Yu, and Y. Wang, "Deep convolutional neural network based on self-distillation for tool wear recognition," *Engineering Applications of Artificial Intelligence*, vol. 132, p. 107851, 2024, doi: 10.1016/j.engappai.2024.107851.

[21] R. Zhao, H. Huang, and L. Mei, "A method for constructing digital twins of CNC machine tools feed systems based on hybrid mechanism-data," *Scientific Reports*, vol. 15, no. 1, p. 32186, 2025, doi: 10.1038/s41598-025-17587-w.

[22] X. Zhang and X. Xie, "A data model-driven prediction and compensation strategy for load disturbances in CNC machine tool feeding systems via digital twin technology," in *Proceedings of the Institution of Mechanical Engineers, Part C: Journal of Mechanical Engineering Science*, Jan. 2025. doi: 10.1177/09544062241309251.

[23] T. Jones and Y. Cao, "Tool wear prediction based on multisensor data fusion and machine learning," *International Journal of Advanced Manufacturing Technology*, vol. 137, no. 9, pp. 5213–5225, 2025, doi: 10.1007/s00170-025-15472-4.

[24] S. Chen *et al.*, "Digital twins for machine tools: a systematic mapping study," *Digital Twin*, vol. 2, no. 4, 2025, doi: 10.1080/27525783.2025.2538727.

[25] ISO/TC 39/SC 2 T, "ISO - ISO 230-2:2014 - Test code for machine tools — Part 2: Determination of accuracy and repeatability of positioning of numerically controlled axes." Geneva, Switzerland, 2017. [Online]. Available: https://www.iso.org/standard/55295.html

BIOGRAPHIES OF AUTHORS



Eman Ebrahim is affiliated with Swiss International University (SIU) and conducts multidisciplinary engineering research spanning autonomous robotics, mechatronic system design, additive manufacturing, mechanical analysis, and experimental validation. In the present study, the author contributed to the mechanical architecture, FDM fabrication strategy, CFD/FEA validation, system integration, experimental methodology, and performance interpretation. Her research centers on developing accessible robotic platforms where mechanical design, embedded control, sensing, and autonomous navigation function as an integrated system. She can be contacted at dr.n.eman@swiss.edu.eu.



Ibrahim Al Souleiman is affiliated with Swiss International University (SIU) and contributes to research involving artificial intelligence, automation, digital systems, and interdisciplinary technology integration. In this study, the author contributed to the robotics software architecture, ROS 2 integration, navigation implementation, experimental validation, and manuscript revision. His work bridges physical mobile platforms with autonomous perception, localization, path planning, and control, emphasizing modular software architectures transferable to broader service-robot applications. He can be contacted at dr.i@swiss.edu.eu.